The Effect of Copper Ions on A53T Alpha-Synuclein Aggregation Implicated in Parkinson's Disease

Maja Keatley
maja@keatley.com

under the direction of
Laurène Adam, MSc
Axel Abelein-Group
Karolinska Institute

Research Academy for Young Scientists
July 13, 2022

Abstract

There are still gaps in the knowledge around the cause of Parkinson's disease. Currently, major research targets alpha-synuclein aggregation leading to the formation of amyloid fibrils. As this protein aggregates, it forms neuro-toxic oligomers which may lead to the formation of Lewy bodies, the known cause of Parkinson's Disease. Several reports have found high concentrations of metal ions in Parkinson's Disease patients, so it is crucial to achieve a further understanding about the effect of metal ions on the disease, and specifically their interaction with alpha-synuclein. This project sought to measure the effect of copper on the aggregation of A53T alpha-synuclein, a Parkinson's Disease related mutation, using ThT aggregation kinetics, an electron microscope, and Circular Dichroism Spectrophotometry. The aggregation of A53T alpha-synuclein with different amounts of copper was measured with a fluorescence machine, and the alpha-synuclein monomer and final fibril structure in absence and presence of copper was looked at with an electron microscope and the secondary structure was measured with a circular dichroism spectrophotometer. The results show that copper accelerates aggregation of A53T alpha-synuclein mutant, and slightly affects the secondary structure of monomers but it does not appear to affect the secondary structure of fibrils. These results provide more detail for understanding how copper might affect alpha-synuclein aggregation in the brain.

Acknowledgements

I would first like to thank Laurène Adam for all her help throughout this project. Her constant guidance, help, and positive presence allowed me to learn and enjoy my experience at Karolinska Institute. Without Laurène, my experience at Karolinska would never had happened, so I thank her for giving me this incredible opportunity. I would also like to thank Axel Abblein, Rakesh Kumar, and Ceclilia Mörman for giving a helping hand and great company throughout this whole project.

I would also like to thank Felix Steinberger Eriksson, Klara Kiselman, och Shirley Lidman for helping me through the writing and editing process.

Thank you to Rays — for excellence for giving me this incredible opportunity and for accepting me into their incomparable program.

Finally, I would like to thank Beijerstiftelsen and Olle Engkvist Stiftelse for partnering with us and giving us this opportunity.

Contents

1 Introduction

Parkinson's disease is an incurable neurodegenerative disorder characterized by the presence of Lewy bodies, which are abnormal deposits of alpha-synuclein, within the brain [1]. Neurodegenerative disorders cause brain decay which can lead to uncontrollable movements, difficulty with balance and coordination, and pain within the body [1]. Parkinson's disease is the second most common neurodegenerative disorder, and it has been predicted that the number of cases will double between 2003 and 2030 [2]. Sporadic cases of Parkinson's disease contribute to about $90\% - 95\%$ of cases, while hereditary cases contribute to $5\% - 10\%$ [2]. Common Parkinson's disease symptoms include dementia, slowed and uncontrollable movements, and pain [3]. Familial Parkinson's disease can be due to a mutation in the alpha-synuclein gene, specifically the mutation A53T where alanine has been replaced by threonine at location 53 on the amino acid chain [2]. This mutation leads to larger than normal oligomers which are toxic to the brain [2].

1.1 Proteins

Proteins play a crucial role in Parkinson's disease, as Lewy bodies are made up of alpha-synuclein proteins [4]. In general, protein molecules are responsible for the structure, function, and regulation of the tissues and organs within the body [4]. In order for proteins to be created, DNA must first be transcribed and translated into amino acids, which are the building blocks of the protein [4].

1.1.1 DNA versus RNA

While DNA and RNA have similar structures, there are certain differences that causes them to have different functions [5]. While both DNA and RNA are linear polymers, DNA consists of deoxyribose sugar while the RNA consists of ribose sugar [5]. Both DNA and RNA have adenine, guanine, and cytosine as nitrogenous bases, but DNA has thymine and RNA has uracil as its fourth base[5]. A key difference between DNA and RNA is

that DNA is a double-stranded helix that cannot leave the nucleus while RNA is a single-stranded helix that can leave the nucleus [5].

1.1.2 Transcription and Translation

Protein synthesis starts by transcribing the DNA into RNA [5]. DNA transcription is when the non-coding strand of the DNA gets transcribed into RNA through the complementary base pairing [5]. Once the RNA is completed and released, it leaves the nucleus to create the amino acid chain [5].

For the RNA to be translated, messenger RNA, ribosomal RNA, and transfer RNA work together to create the amino acid chain or the primary structure of the protein, as shown in figure 1 [5].

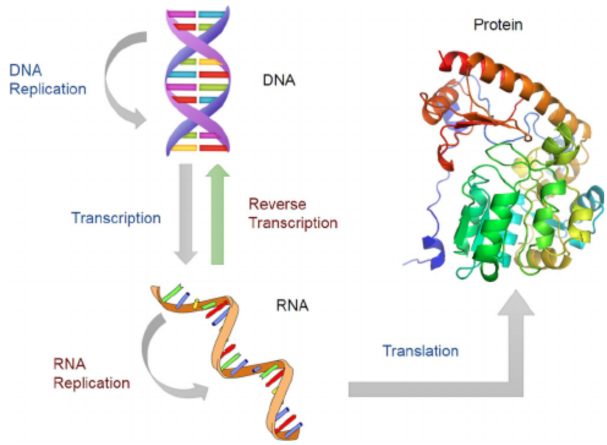

Figure 1: Illustration of the process of DNA translation and transcription.[6]

1.1.3 Protein Structure

Proteins have four different structures. The primary structure is the amino acid chain [4]. The secondary structure is the folding of the amino acid chain into alpha-helices, beta-sheets, and random coils based on the charge and polarity of the different amino acids [4]. The tertiary structure is how those beta-sheets, alpha-helices, and random coils fold together to create the final shape of one protein molecule [4]. This is also affected by charge and polarity [4]. Some proteins have the ability to form quaternary structures,

which is when different protein monomers react to form multimers [4].

1.2 Protein Purification and Analysis

As proteins are the main working molecules in our body, they are widely studied by researchers to gain further understanding about their structures and functions in healthy tissues as well as in disease [4].

1.2.1 Protein Production in the Lab

Proteins are produced in the lab through the use of plasmid DNA and bacteria [7]. Plasmids are small circular self-replicating DNA often found in bacteria [7]. To use the plasmids in the lab they are first removed from the bacteria, and, afterword, the DNA of a target protein is injected within the plasmid DNA through the use of a restriction enzymes [8]. Restriction enzymes lacerate a precise location on the DNA where the desired DNA will be combined in [8]. Thus, the DNA ligase binds the DNA from the wanted protein to the plasmid DNA, which is placed into, commonly, E. Coli bacteria to replicate [8].

1.2.2 Protein Purification

Bacteria synthesize endogenous proteins at the same time as the desired protein[9]. Thus, to purify the protein of interest, several steps of purification are needed: lysis, chromatography methods, and a purity check [9]. Based on the chemical and physical properties of the protein of interest, different chromatography methods are used, so these steps are for alpha-synuclein specifically [9].

First, the cell membranes are punctured through chemical or physical lysis [9]. This allows the cytosolic proteins, including the protein of interest, to exit the bacteria [9]. Then the sample must be placed into a centrifuge, in order to separate the cell debris from soluble components [9].

After centrifugation, the soluble mixture runs through anion exchange chromatography [10]. Anion exchange chromatography uses a positively charged resin which attracts

negative ions to the resin, while allowing positively charged ones to pass through [10]. The positively charged ions that flow through are called the run off [10]. Once the run off has passed through, a buffer with a high salt concentration is used to wash away the negatively charged ions with the desired protein [10]. This technique can be used only if your protein has a net negative charge [10].

After anion exchange chromatography, for this experiment, the sample goes through reverse phase chromatography [11]. Reverse phase chromatography uses alkyl chains, which are chains of hydrogen and carbon atoms covalently bonded to stationary phase molecules, to divide the mixture based on polarity, due to the alkyl chains affinity for low polar molecules [11].

Afterword, the remaining sample is lyophilised and loaded into a size exclusion chromatography column which is used to divide molecules based on their size [11, 12]. In size exclusion chromatography, the tube is filled with porous beads which allow large proteins to fall through quicker than small proteins [12]. The large proteins are usually dimers or polymers, and the small proteins are usually monomers [12]. In the chromatogram, the UV signal at $280nm$ will indicate that proteins have eluted [12].

1.2.3 Checking the Purity of Proteins

Then the purity of the sample is verified [13]. One common way of doing this is through the use of sodium dodecyl sulfate-polyacrylamide gel electrophoresis, also known as SDS PAGE [13]. Electrophoresis is the separation of macromolecules on an electric field [13]. For proteins specifically, SDS PAGE is a common variation of electrophoresis because it uses discontinuous polyacrylamide gel, where the anion in the gel is different from the common anion in the buffer, so it creates good band resolution and definition [13]. Additionally, it uses sodium dodecyl sulfate or SDS which easily denatures the proteins [13]. The negative charge on SDS destroys most of the protein's structure and also allows the protein to be negatively charged so it will be pulled towards a positive anode [13]. Polyacrylamide gels allow smaller molecules to move through the gel easier than larger

molecules [13]. This allows one to analyze the length of the polypeptides based on how far the molecule goes down the gel in comparison to the protein ladder. An example protein ladder is shown in figure 2 [13]. Alpha-synuclein, specifically, has a length of 14 kilodaltons.

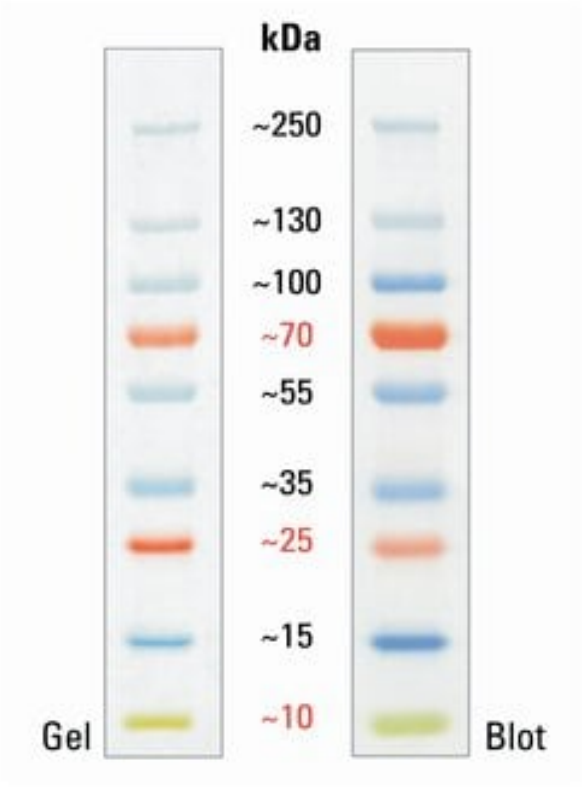

Figure 2: Protein ladder used in SDS gel analysis.[6]

1.3 Alpha-Synuclein

Alpha-synuclein is a small acidic protein, and it accounts for $0.5\% - 1\%$ of brain proteins [14].

1.3.1 Alpha-synuclein Structure

Alpha-synuclein is made up of three major sections: the amphipathic N terminal fragment, the acidic C terminal fragment, and the hydrophobic non-amyloid β component [15]. The N terminal fragment controls membrane interactions and lipid bindings. It is important to note that the A53T mutation is located in the N terminal fragment [15]. The

C-terminal controls interactions with proteins, ligands, and metal ions [3]. The final part, the non-amyloid β component, is incharge of the protein aggregation and the formation of the beta-sheet secondary structure [16]. It is also important to note that SNCA is the gene that codes for alpha-synuclein, and it is the gene where the A53T mutation is coded [17].

Alpha-synuclein proteins which are found in the cytosol are often unorganized and stretched-out, but alpha-synuclein proteins which are bound to cellular membranes clusters to form a helix composed of two alpha-synuclein monomers [18].

Normally, the secondary structure of alpha-synuclein fibrils are highly beta-sheet dominant while the secondary structures of alpha-synuclein monomers are usually random coils [18].

Alpha-synuclein has many different functions including suppression of apoptosis, regulation of glucose levels, chaperone activity, antioxidation, neural differentiation, and much more including the regulation of synaptic vesicles, and glucose level regulations [18].

1.3.2 Mutations in the SNCA Gene Cause Parkinson's Disease

Both alpha-synuclein mutations A30P and A53T have previously been shown to promote increased formation of large oligomers, but the specific mutation used in this research was the A53T mutation.[19]

1.4 Parkinson's Disease

Parkinson's Disease is caused by the collection of alpha-synuclein molecules into Lewy bodies [20]. Lewy bodies form when alpha-synuclein monomers aggregate and form clusters [20].

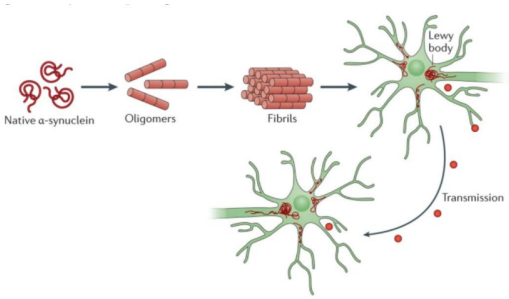

Figure 3: The underlying pathogenesis of Parkinson's Disease

[21]

As shown in figure 3, when alpha-synuclein is aggregating, it develops into oligomers which are the most toxic for the brain out of alpha-synuclein monomers, oligomers, and fibrils [22]. These oligomers often clump and lead to the death of dopaminergic neurons [22]. A decrease in dopamine causes an imbalance in pathways within the basal ganglia which leads to common symptoms of Parkinson's Disease, such as bradykinesia [22]. Recent findings suggest that Parkinson's Disease is further encouraged by the cell-to-cell transmission of the misfolded alpha-synucleins, but this is yet to be proven [22].

1.5 Aggregation Mechanisms

In order for alpha-synuclein monomers to become fibrils, it must first go through nucleation which is also known as aggregation. The first nucleation is self-assembly in order to form clusters or groups [23]. When going through nucleation into alpha-synuclein fibrils the alpha-synuclein become oligomers, hence, in order to limit the chances of Parkinson's disease caused by nucleation, one would want to shorten the aggregation time or, preferably, stop aggregation all together [23].

1.6 Role of Copper

Copper affects the functional roles of the normal brain through playing a role in antioxidative radical defense, free radical defense, energy metabolism, iron metabolism,

neurotransmitter synthesis, and neuropeptide synthesis [24]. In recent years, copper has been found to be capable of binding to alpha-synuclein in both soluble and membrane bound states [24]. When alpha-synuclein is bound to copper it often becomes a toxic oligomer [24].However, the exact way copper affects Parkinson's Disease has not been established [25].

Alpha-synuclein has a structure that allows it to bind to metal ions at many different locations throughout the protein [25]. In previous studies, metal ions have proved to play a role in accelerating misfolding within alpha-synuclein [25]. Additionally, people with neurodegenerative diseases have previously been found to have an imbalance in metal ions in their tissue [25]. Other studies have also shown that metals ions affect the speed of aggregation for Parkinson's Disease [25]. For example, Keskitalo et al. conveyed that copper speeds up aggregation for the wild type of alpha-synuclein [26].

In a study by Raisa et al., in 2005, it was concluded that copper was the most efficient metal ion at enhancing alpha-synuclein oligomer formation [27].

1.7 Aim of Study

The aim of this project was to study the effect of Cu(II) on the A53T alpha-synuclein protein.

2 Method

This study aims to measure pure A53T alpha-synuclein aggregation rates with different concentrations of copper ions and to analyze the different monomer and fibril structures of A53T alpha-synuclein when affected by copper.

2.0.1 Checking Protein Purity

Before performing aggregation kinetics, a pure protein sample is needed. Prior to my arrival, the A53T mutant protein had been purified and the samples collected during the

final stage of purification were loaded on an SDS PAGE gel to check its purity. Several samples from the purification, described in the legend of figure 6, have been loaded on an SDS PAGE gel (420%, BioRad) with 1X loading buffer containing SDS. The samples were then boiled for ten minutes. The gel was then run for 20 minutes at $300V$ and further stained with Coomassie blue during one hour and, afterword, destained with water.

2.1 ThT Aggregation Kinetics of A53T in Presence of Copper

For this experiment, we used a Flourstar 52 machine. The Flourstar 52 is a microplate reader that uses ultra-fast UV/vis spectrometer or filters for absorbance in order to detect fluorescence from a microplate. The machine often uses the fluorescing dye Thioflavin T to bind to alpha-synuclein fibrils beta-sheets when the protein aggregates.

First a table was made in order to calculate the volume of everything that was going into each of the seven samples. Copper's percentage was in comparison to alpha-synuclein's concentration of $70M$.

Table 1: Concentration and volumes for wells in well plate for Flourstar 52, all concentrations and volumes calculated with the equation $C_1V_1 = C_2V_2$

Samples	$\alpha - Syn$ (μM)	$\alpha - Syn$ (μL)	Cu(II) (μM)	Cu(II) (μL))
+ 0% Cu(II)	70	77.2	0	0
+ 5% Cu(II)	70	77.2	3.5	1.1
+ 10% Cu(II)	70	77.2	7	2.1
+ 25% Cu(II)	70	77.2	17.5	5.3
+ 50% Cu(II)	70	77.2	35	10.5
+75% Cu(II)	70	77.2	52.5	15.8
+100% Cu(II)	70	77.2	70	21
Samples	ThT (μL)	20 mM NaP pH 7.4 (μL)	Total (μL)	
+ 0% Cu(II)	3	69.8.2	150	
+ 5% Cu(II)	3	68.8	150	
+ 10% Cu(II)	3	67.7	150	
+ 25% Cu(II)	3	64.6	150	
+ 50% Cu(II)	3	59.3	150	
+75% Cu(II)	3	54.1	150	
+100% Cu(II)	3	48.8	150	

A 384 well microplate was gathered. Two ca. one mm glass beads were tweezed into each of the first 48 cells on the microplate. Each sample was prepared in an eppendorf tube based on the values in table 1. First a sample with just three microliters of ThT and 147μL of $20mMNaPpH7.4$ buffer was placed in well one through six to act as a base line. Then, the sample with zero percent Cu(II) was mixed and then 20μL were placed into cells seven through twelve on the well microplate because each sample had six replicates or tests. The above step was repeated for all the rest of the tubes but they were placed in the respective cells with tube two being in wells thirteen through eighteen and so on. Subsequently, the cell plate was covered with plastic and rolled over in order to

ensure that there was no air in the wells. The cell plate was then placed into a Flourstar 52 machine, the fluorescence measuring machine, for a week at $37°C$. The machine measured the fluorescence every 10 minutes between each cycle of orbital shaking.

2.2 Electron Microscopy Imaging

Five microliters of diluted solution was applied on 200 mesh formvar coated nickel grid and excess solution was removed using blotting paper after 10 min of incubation. It was then washed twice with $10l$ MQ water and stained with one percent uranyl formate for five minutes. Extra stain was blotted with blotting paper, and after it was air-dried. Transmission electron microscopy (FEI Tecnai 12 Spirit BioTWIN, operated at $100kV$) was performed for analysis of fibril morphology using $2k2k$ Veleta CCD camera (Olympus Soft Imaging Solutions, GmbH, Münster, Germany). Three to ten images were recorded of each sample randomly.

2.3 Circular Dichroism Spectrophotometry (CD)

For this experiment, a Circular Dichroism Spectrophotometer was used. A Circular Dichroism Spectrophotometer measures the interaction of molecules with light that is circularly polarized [28]. In linearly polarized light the electron magnetic field magnitude changes but the axis does not. Electron magnetic fields are fields caused by the moving of electrons [28]. In circularly polarized light both the axis and the magnitude changes [28]. In circularly polarized light, there are two waves where one of the waves is in the middle or at zero when the other is at its maximum [28]. This means that the light has two different plane waves with equal amplitude but they differ in phase by 90 degrees [28]. This causes the electromagnetic field to be polarized in different directions at the same time which ends up creating a circle [28]. When the wave is rotating in a clockwise direction it is right handed, and when the wave is rotating in a counterclockwise direction it is left handed [28]. Different molecules absorb circularly polarized light in either a left-

handed or right-handed way based on the molecule's symmetry [28]. When the molecule absorbs left and right handed light, the different degrees result in an electric field vector that traces out ellipses [28].

Figure 4 shows the different types of polarized lights on different axis.

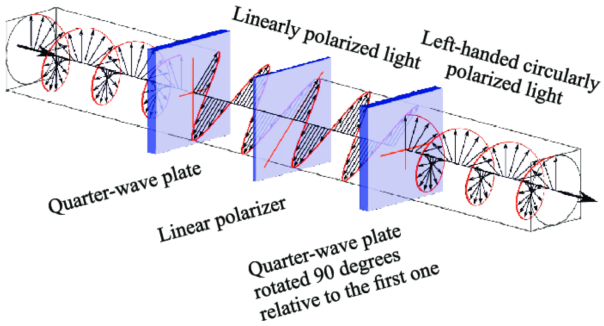

Figure 4: Illustration demonstrating the difference between left, right, and linear polarized light

Circular Dichroism Spectrophotometry can be used to study protein folding, form, and function [28]. Specifically, a circular dichroism spectrophotometer can be used to analyze the secondary structure of proteins [28]. The two bands 190 and the band between

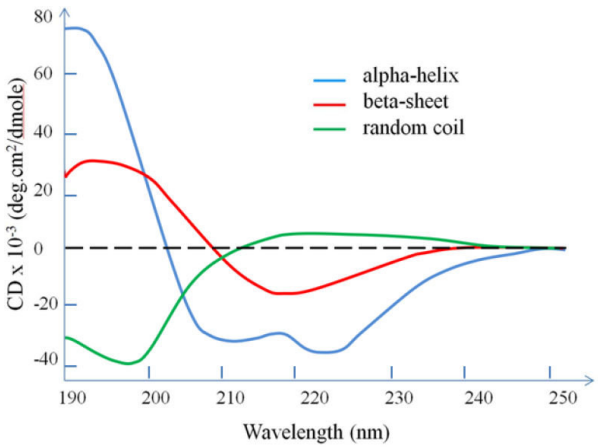

Figure 5: Circular Dichroism Spectrophotometry graph results for different secondary structures. The y-axis shows the circular dichroism with the left circular dichroism being positive and the right circular dichroism being negative. The x-axis represents the wavelength of the different lights that got directed towards the molecule [29]

$210 - 220$ help estimate the secondary structure components of the protein [28]. All of the different types of the secondary structure including beta-sheets, alpha-helices, and

random coils, have different CD spectra, as shown in figure 5, so one can compare the normal graph produced by the secondary structures to the graph of the current protein being analyzed in order to analyze the proteins secondary structure [28]. If a molecule contains chiral chromophores then either the left circularly polarized luminance will be absorbed more or less then the right circularly polarized luminance[28]. If the right light is absorbed more it appears negative on the circular dichroism graph, and if the left light is absorbed more it appears positive on the circular dichroism graph [28].

The following method was used in order to measure the secondary structure of the A53T alpha-synuclein monomers and fibrils in presence of copper.

2.3.1 CD of A53T alpha-synuclein in presence of copper

First, a table was made in order to calculate all the volumes needed for the experiment. In the table the percentage of the copper was compared to the amount of alpha-synuclein, so 100% copper meant that the molar concentration of copper was equal to the molar concentration of A53T alpha-synuclein (ratio 1 : 1).

Table 2: Concentrations and Volume of Cu(II) and A53T $\alpha - Syn$ with CU(II) percentage in comparison to A53T $\alpha - Syn$. Alpha-synuclein final consecration is 70 $\mu M and copper s percentage is in comparison to that 70 \mu M$

Samples	$\alpha - Syn$ (μM)	$\alpha - Syn$ (μL)	Cu(II) (μM)	Cu(II) (μL)	20 mM NaP pH 7.4 (μL)
+ 0% Cu(II)	5	7.4	0	0	192.6
+ 10% Cu(II)	5	7.4	0.5	0.2	192.4
+ 25% Cu(II)	5	7.4	1.25	0.5	192.1
+ 50% Cu(II)	5	7.4	2.5	1	191.6
+75% Cu(II)	5	7.4	3.75	1.5	191.1
+100% Cu(II)	5	7.4	5	2	190.6

All the different samples were prepared in eppendorf tubes based on the values from table 2. Next, 150μL of the pure buffer was placed into the CDS flask in order to measure

a base line. The flask was then placed into the CDS machine at $25°C$. The CDS machine was then run for about 15 minutes or until the machine had read the sample five times completely. The previous four steps were repeated for the six samples.

2.3.2 CD of A53T Alpha-Synucein Fibrils in Presence of Copper

First, the volume of one well of each sample, besides the 5% sample, used in the Fluorescence machine were measured. Consequently, the equation $C_1V_1 = C_2V_2$ was used in order to get the final concentration of alpha-synuclein from $70\mu M$ to five μM. Then the samples were prepared based on the values in table 3.

Table 3: Concentrations and volumes for fibril CD Spectrophotometry, numbers calculated with equation $C_1V_1 = C_2V_2$

Samples	original $\alpha - Syn$ (μM)	well sample (μL)
+ 0% Cu(II)	70	10.5
+ 10% Cu(II)	70	11.5
+ 25% Cu(II)	70	12
+ 50% Cu(II)	70	11
+75% Cu(II)	70	12.5
+100% Cu(II)	70	13.5
20 mM NaP pH 7.4 (μL)	final $\alpha - Syn$ (μM)	Total (μL)
136.5	5	147
149.5	5	161
156	5	168
143	5	154
162.5	5	175
175.5	5	189

After the base line was run as described in the section above, $150\mu L$ of the zero percent copper sample was placed into the flask for the Circular Dichroism Spectrophotometer

machine. The flask was then placed into the machine and read five times at 25°C. The above two steps were repeated for all six samples.

3 Results

In general the higher the concentration of Cu(II) the quicker the aggregation speed. Alpha-synuclein alone had the slowest aggregation speed, and the sample with 75% Cu(II) had the quickest aggregation speed. The electron microscope images only showed fibrils in the 5% example, so no conclusions could be drawn. Finally, Cu(II) does not affect the secondary structure of alpha-synuclein monomers and fibrils, but the results indicate that Cu(II) interacts with A53T alpha-synuclein monomers.

3.1 Protein purification

As illustrated in figure 6, the protein used in this experiment was pure alpha-synuclein because the line was around 14 kiloDalton which is the expected length for alpha-synuclein.

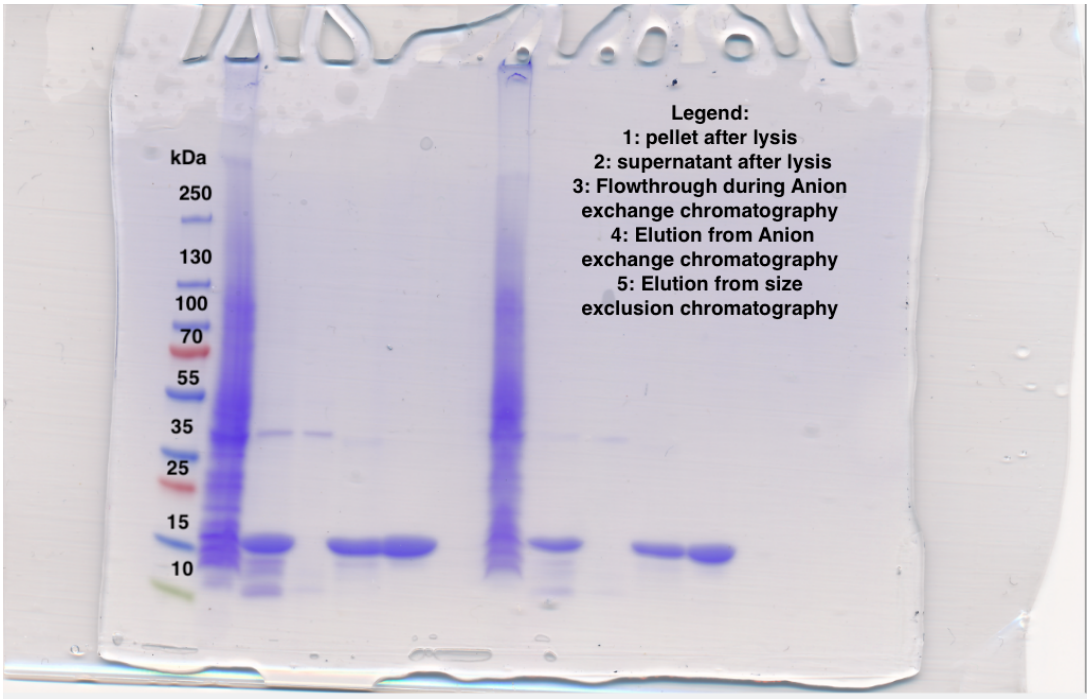

Figure 6: SDS PAGE Gel of A53T alpha-synuclein pure protein.

3.2 ThT aggregation kinetics of A53T alpha-synuclein mutant in presence of copper

Figure 7 illustrates the average of all the wells for each sample compared on a graph. This is the untouched data in order to give the raw results. A53T alpha-synuclein alone is the slowest aggregation and A53T alpha-synuclein with 75% copper was the fastest aggregation.

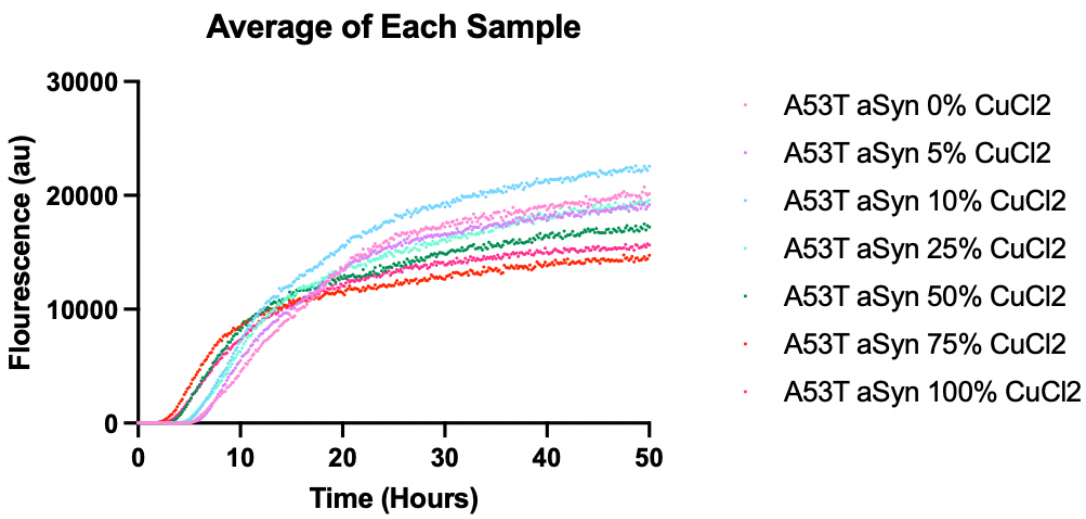

Figure 7: Average kinetics data of A53T alpha-synuclein in presence of different concentration of Cu(II)

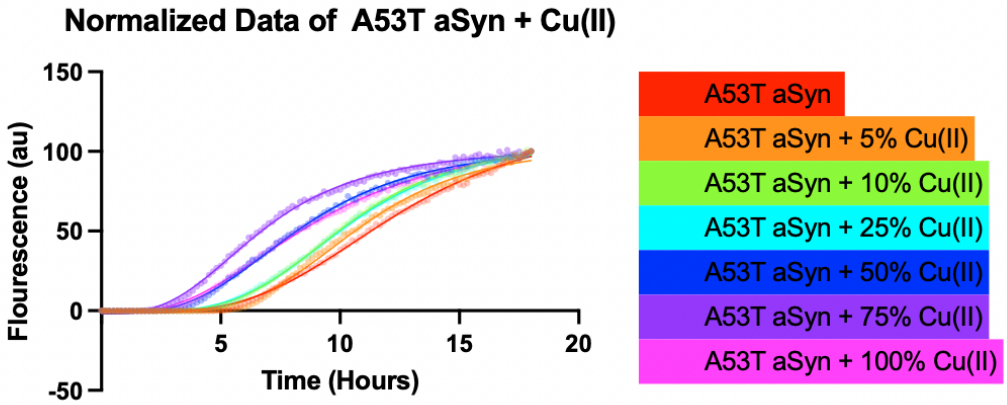

Figure 8: Normalized kinetics data of A53T alpha-synuclein in presence of different concentration of Cu(II)

Figure 8 illustrates the normalized data of the kinetics in order to easily compare the different aggregation rates. The slowest aggregation rate was alpha-synuclein alone, while the fastest aggregation rate was 75% Cu(II).

More tables showing averaged aggregation kinetics for each sample and each replicate in each sample are provided in Appendix A.

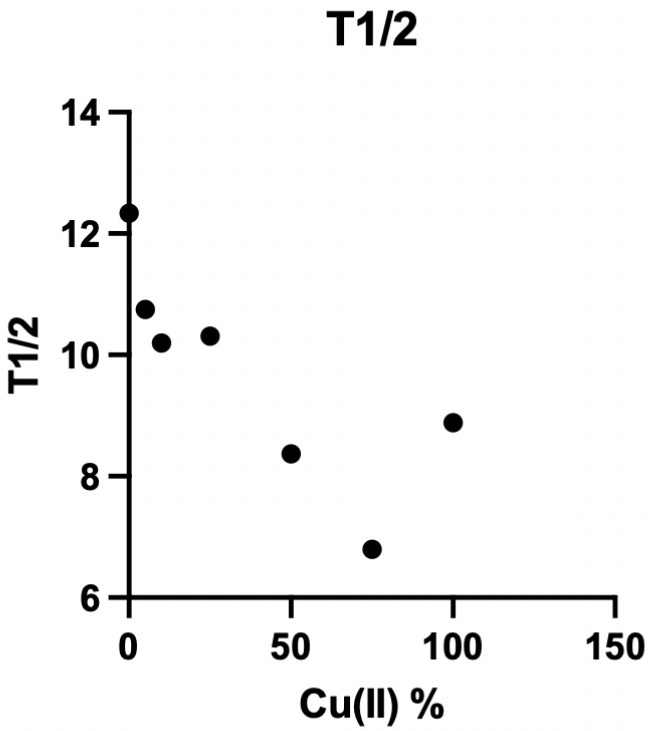

Figure 9: Aggregation half time of A53T alpha-Synuclein (70M)as a function of different concentrations of Cu(II)

Figure 9 illustrates the T1/2 value of the different samples. The T1/2 value is the time when the sample is halfway through aggregation. These numbers allow an easy and numerical way to compare aggregation half time. Alpha-synuclein alone has the largest T1/2 value at around 12 while the sample with alpha-synculein and 75% copper has the lowest T1/2 value around seven. The lower the T1/2 value the quicker the aggregation.

3.3 Electron Microscopy Imaging

Figure 10 below illustrates alpha-synuclein fibrils alone, with 5% copper, and with 10% copper.

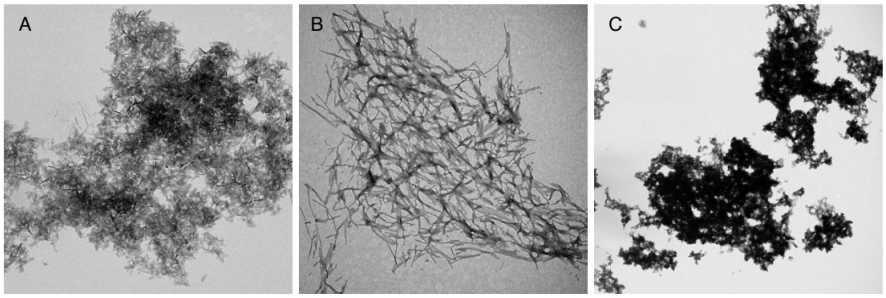

Figure 10: A53T alpha-synuclein fibrils under an electron microscope. Image (a) shows A53T alone. Image (b) shows A53T alpha-synuclein with 5% copper, and image (c) shows A53T alpha-synuclein with 10% copper

In figure 10, the only one that shows the fibrils is the 5% photo, the others have black masses that could either be contamination or groups of fibrils. Little to no conclusions can be drawn from these images.

3.4 Circular Dichroism Spectrophotometry

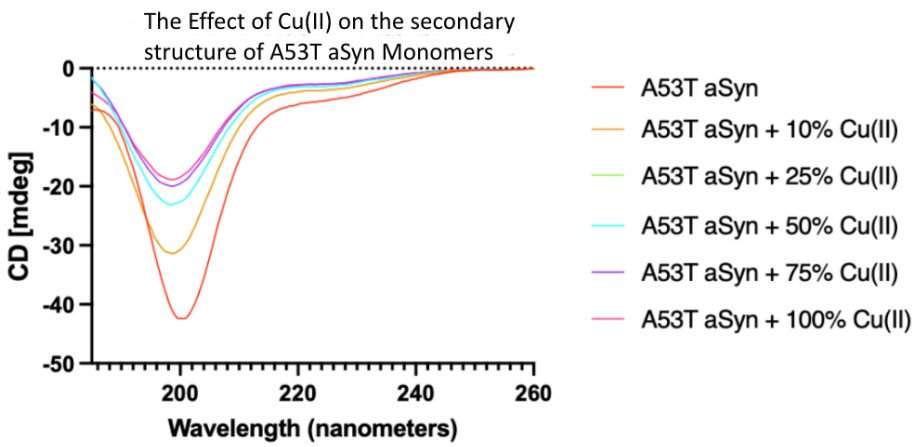

Figure 11: The CD measurements of absorbance compared to light wavelengths reflected onto monomers of A53T alpha-synuclein affected by different amounts of Cu(II).

As copper is added to A53T alpha-synuclein monomers the CD intensity decreases. The overall structure of all the samples is still a random coil, or unstructured loops, but the intensity is not the same, as shown in figure 11.

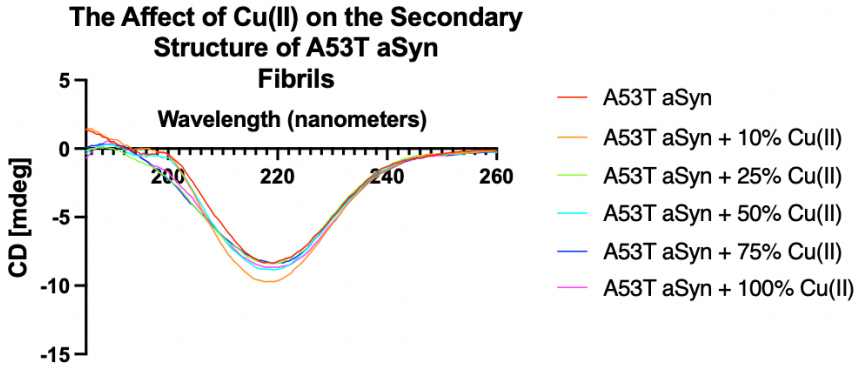

Figure 12: The CD measurements compared to light wavelengths of fibrils of A53T alpha-synuclein affected by different amounts of Cu(II).

The secondary structure of A53T alpha- synuclein fibril are as expected: beta-sheets. The signal remains relatively the same when aggregated with Cu(II), as shown in figure 12.

4 Discussion

The following section will first focus on the results and analyze them. Then it will go into future studies and a final conclusion.

4.1 Result Analysis

The following section will focus on analyzing the results. It will analyze and discuss the results from the fluorescence machine, the electron microscope photos, and the Circular Dichroism Spectrophotometer graphs.

4.1.1 Fluorescence

As the concentration of copper increases so does the aggregation speed. This is illustrated through the steeper slope of the samples with higher Cu(II) concentration, in both

figure 7 and figure 8. Additionally, this trend is conveyed in the lower T1/2 values in figure 9, where the 75% CU(II) sample had a T1/2 value of about seven, and the alpha-synuclein alone sample had a T1/2 value of about 12. This trend was also consistent with the wild type of alpha-synuclein which had been previously run at the same lab. The only sample that diverged from this trend was the 100% Cu(II) sample which had a slower aggregation rate than both the 50% Cu(II) sample and the 75% Cu(II) sample, shown by the T1/2 value of about nine. This could be due to experimental errors, or it could show that too much copper slows down the aggregation time. The experimental error that could have caused this issue was the amount of air left in the well plate, which led to evaporation. Each sample went from 20L to around 10L implying that evaporation had occurred and, therefore, a change in concentration within the samples had also occurred.

4.1.2 Electron Microscope

No definite conclusion can be drawn from the electron microscope photos because only the five percent Cu(II) sample showed any fibrils. The other two samples showed big black masses which could have been due to contamination or too high concentration in the sample, meaning that the fibrils were clumped together. There could have also been too little concentration, so no fibrils were present in the sample and were, instead, still stuck to the well surfaces in the plate.

4.1.3 Circular Dichroism Spectrophotometry

Comparison of Circular Dichroism Spectrophotometry data to the normal curve in figure 5 of different secondary structures of proteins, showed that the A53T alpha-synuclein monomers with all percentages of copper had a random coil structure. This is normal for A53T alpha-synuclein monomers because normally they have little to no structure until they form fibrils. As copper was added there seemed to be some change in the graphs in a positive y-axis direction, for example the 100% sample had a minimum around negative 20 while the alpha-synuclein alone sample has a minimum around negative 45, and

this could convey that there is interaction between the alpha-synuclein monomers and the CU(II). The one inconsistency within this data was that the 10% sample and the 25% sample resulted in identical graphs, but this could be because the 10% sample was probably run twice.

For the fibrils, the samples are consistent. They are all similar to the beta-sheet graph presented in the introduction, and also the beta-sheet structure of normal alpha-synuclein fibrils. This means that copper probably does not have any effect on the final secondary structure of the A53T alpha-synuclein fibrils if copper is added during the aggregation.

4.2 Future Studies

Overall, additional research on the structure of both the fibrils and monomers of A53T alpha-synuclein and the structure of Cu(II) could help us understand more about the role of copper in Parkinson's Disease and, at a later stage, prevent the creation of Lewy bodies in Parkinson's Disease.

There should be studies on how to stop copper from binding to alpha-synuclein so that it does not increase or encourage the formation of alpha-synuclein oligomers during aggregation. This research should include more experiments on how copper binds to alpha-synuclein by more resolutive methods such as Nuclear Magnetic Resonance, and how that binding could be stopped either through other substances or ways to affect the actual binding structure.

Furthermore, there should be research on copper's effect on the secondary structure of the monomer of alpha-synuclein, and how that could be used to stop the binding and therefore the encouraged aggregation.

In the field, researchers are still debating whether copper binds to alpha-synuclein during the aggregation or after alpha-synuclein aggregates. There is still a lot to do to understand more about the general metal ions roles in Parkinson's Disease.

4.3 Conclusion

According to this study, Cu(II) speeds up the aggregation of A53T alpha-synuclein but does not affect the general secondary structure of either the monomers or the fibrils. In general, this research helps further the knowledge of the cause of Parkinson's disease and could be used to help create medicine or a cure for Parkinson's Disease in the future.

References

[1] Guerrero-Ferreira R, Taylor NM, Mona D, Ringler P, Lauer ME, Riek R, et al. Cryo-EM structure of alpha-synuclein fibrils. elife. 2018;7.

[2] Davie CA. A review of Parkinson's disease. British medical bulletin. 2008;86(1):109-27.

[3] Mehra S, Sahay S, Maji SK. α-Synuclein misfolding and aggregation: Implications in Parkinson's disease pathogenesis. Biochimica et Biophysica Acta (BBA)-Proteins and Proteomics. 2019;1867(10):890-908.

[4] Schmidt B. Proteins: Structure and Function. By David Whitford.. Wiley Online Library; 2006.

[5] Alberts B, Johnson A, Lewis J, Raff M, Roberts K, Walter P. From DNA to RNA. In: Molecular Biology of the Cell. 4th edition. Garland Science; 2002. .

[6] Qin Y, Yalamanchili HK, Qin J, Yan B, Wang J. The current status and challenges in computational analysis of genomic big data. Big data research. 2015;2(1):12-8.

[7] Esser K, Kück U, Lang-Hinrichs C, Lemke P, Osiewacz HD, Stahl U, et al. Plasmids of eukaryotes: fundamentals and applications. 2012.

[8] Micklos DA, Freyer GA, et al. DNA science; a first course in recombinant DNA technology. Cold Spring Harbor Laboratory Press; 1990.

[9] Bernhardt TG, Wang N, Struck DK, Young R. Breaking free:"protein antibiotics" and phage lysis. Research in microbiology. 2002;153(8):493-501.

[10] Powers AE, Patel DS. Expression and purification of untagged α-synuclein. In: Alpha-Synuclein. Springer; 2019. p. 261-9.

[11] Molnar I, Horváth C. Reverse-phase chromatography of polar biological substances: separation of catechol compounds by high-performance liquid chromatography. Clinical chemistry. 1976;22(9):1497-502.

[12] Barth HG, Jackson C, Boyes BE. Size exclusion chromatography. Analytical chemistry. 1994;66(12):595-620.

[13] Schägger H, Aquila H, Von Jagow G. Coomassie blue-sodium dodecyl sulfate-polyacrylamide gel electrophoresis for direct visualization of polypeptides during electrophoresis. Analytical biochemistry. 1988;173(1):201-5.

[14] Tofaris GK. Initiation and progression of α-synuclein pathology in Parkinson's disease. Cellular and Molecular Life Sciences. 2022;79(4):1-11.

[15] Choong CJ, Mochizuki H. Neuropathology of α-synuclein in Parkinson's disease. Neuropathology. 2022;42(2):93-103.

[16] Au KLK, Wong JK, Tsuboi T, Eisinger RS, Moore K, Lemos Melo Lobo Jofili Lopes J, et al. Globus pallidus internus (GPi) deep brain stimulation for Parkinson's disease: expert review and commentary. Neurology and Therapy. 2021;10(1):7-30.

[17] Yoshino H, Hirano M, Stoessl AJ, Imamichi Y, Ikeda A, Li Y, et al. Homozygous alpha-synuclein p. A53V in familial Parkinson's disease. Neurobiology of aging. 2017;57:248-e7.

[18] Emamzadeh FN. Alpha-synuclein structure, functions, and interactions. Journal of research in medical sciences: the official journal of Isfahan University of Medical Sciences. 2016;21.

[19] Ingelsson M. Alpha-synuclein oligomers—neurotoxic molecules in Parkinson's disease and other Lewy body disorders. Frontiers in neuroscience. 2016;10:408.

[20] Froula JM, Castellana-Cruz M, Anabtawi NM, Camino JD, Chen SW, Thrasher DR, et al. Defining α-synuclein species responsible for Parkinson's disease phenotypes in mice. Journal of Biological Chemistry. 2019;294(27):10392-406.

[21] Kingwell K. Zeroing in on neurodegenerative [alpha]-synuclein. Nature Reviews Drug Discovery. 2017;16(6):371-4.

[22] Vascellari S, Manzin A. Parkinson's Disease: A Prionopathy? International Journal of Molecular Sciences. 2021;22(15):8022.

[23] Cookson MR, van der Brug M. Cell systems and the toxic mechanism (s) of α-synuclein. Experimental neurology. 2008;209(1):5-11.

[24] Scheiber IF, Mercer JF, Dringen R. Metabolism and functions of copper in brain. Progress in neurobiology. 2014;116:33-57.

[25] Binolfi A, Rasia RM, Bertoncini CW, Ceolin M, Zweckstetter M, Griesinger C, et al. Interaction of α-synuclein with divalent metal ions reveals key differences: A link between structure, binding specificity and fibrillation enhancement. Journal of the American Chemical Society. 2006;128(30):9893-901.

[26] Keskitalo S, Farkas M, Hanenberg M, Szodorai A, Kulic L, Semmler A, et al. Reciprocal modulation of Aβ42 aggregation by copper and homocysteine. Frontiers in aging neuroscience. 2014;6:237.

[27] Rasia RM, Bertoncini CW, Marsh D, Hoyer W, Cherny D, Zweckstetter M, et al. Structural characterization of copper (II) binding to α-synuclein: Insights into the bioinorganic chemistry of Parkinson's disease. Proceedings of the National Academy of Sciences. 2005;102(12):4294-9.

[28] Whitmore L, Wallace BA. Protein secondary structure analyses from circular dichroism spectroscopy: methods and reference databases. Biopolymers: Original Research on Biomolecules. 2008;89(5):392-400.

[29] Wei Y, Thyparambil AA, Latour RA. Protein helical structure determination using CD spectroscopy for solutions with strong background absorbance from 190 to 230 nm. Biochimica et Biophysica Acta (BBA)-Proteins and Proteomics. 2014;1844(12):2331-7.

A Fluorescence Graphs

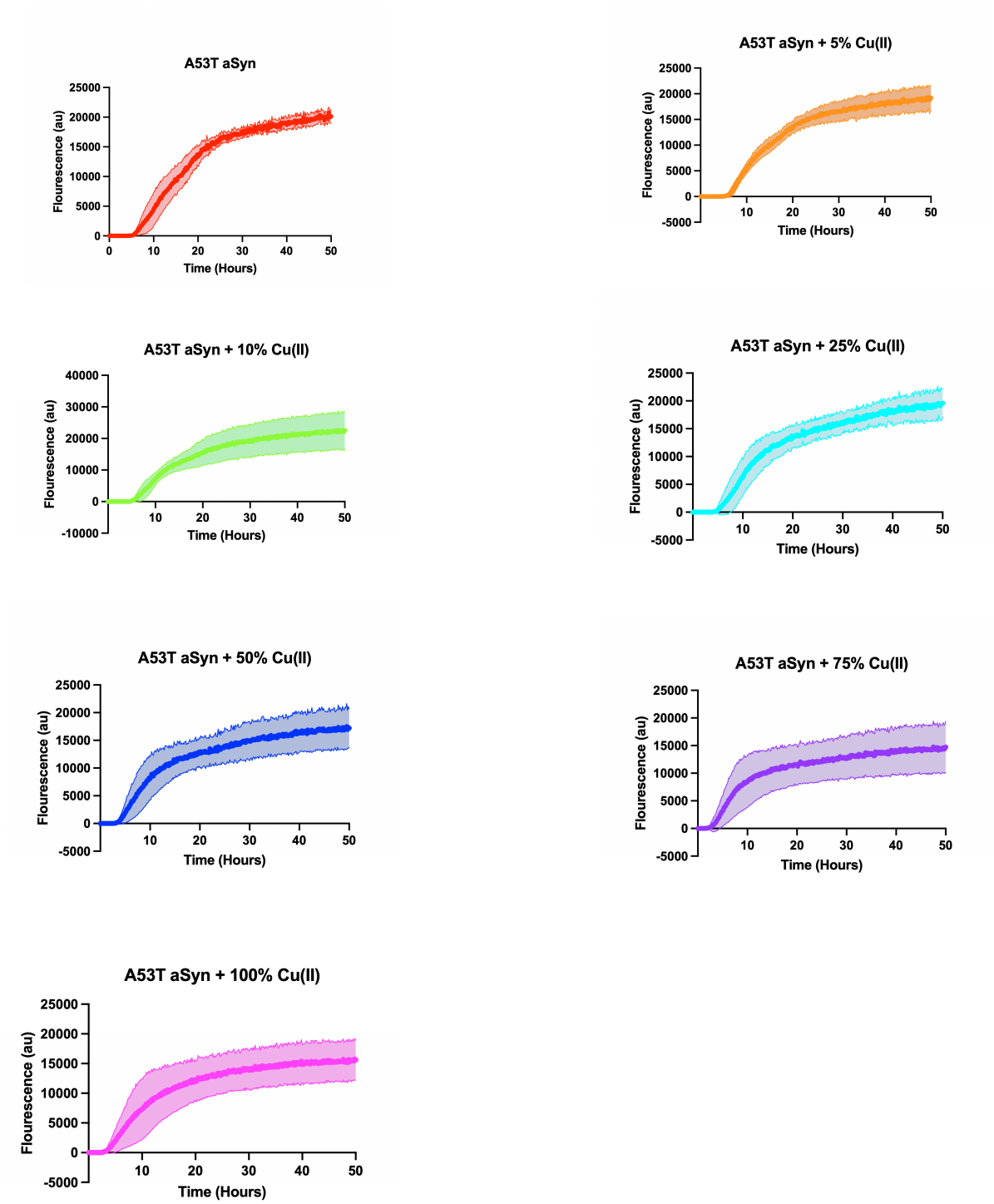

Figure 13: ThT aggregation kinetics with A53T alpha-synuclein and Cu(II). Solid line in middle represents average. The two outer lines with the solid color in between represent the the distribution of the samples fluorescence at that time point.

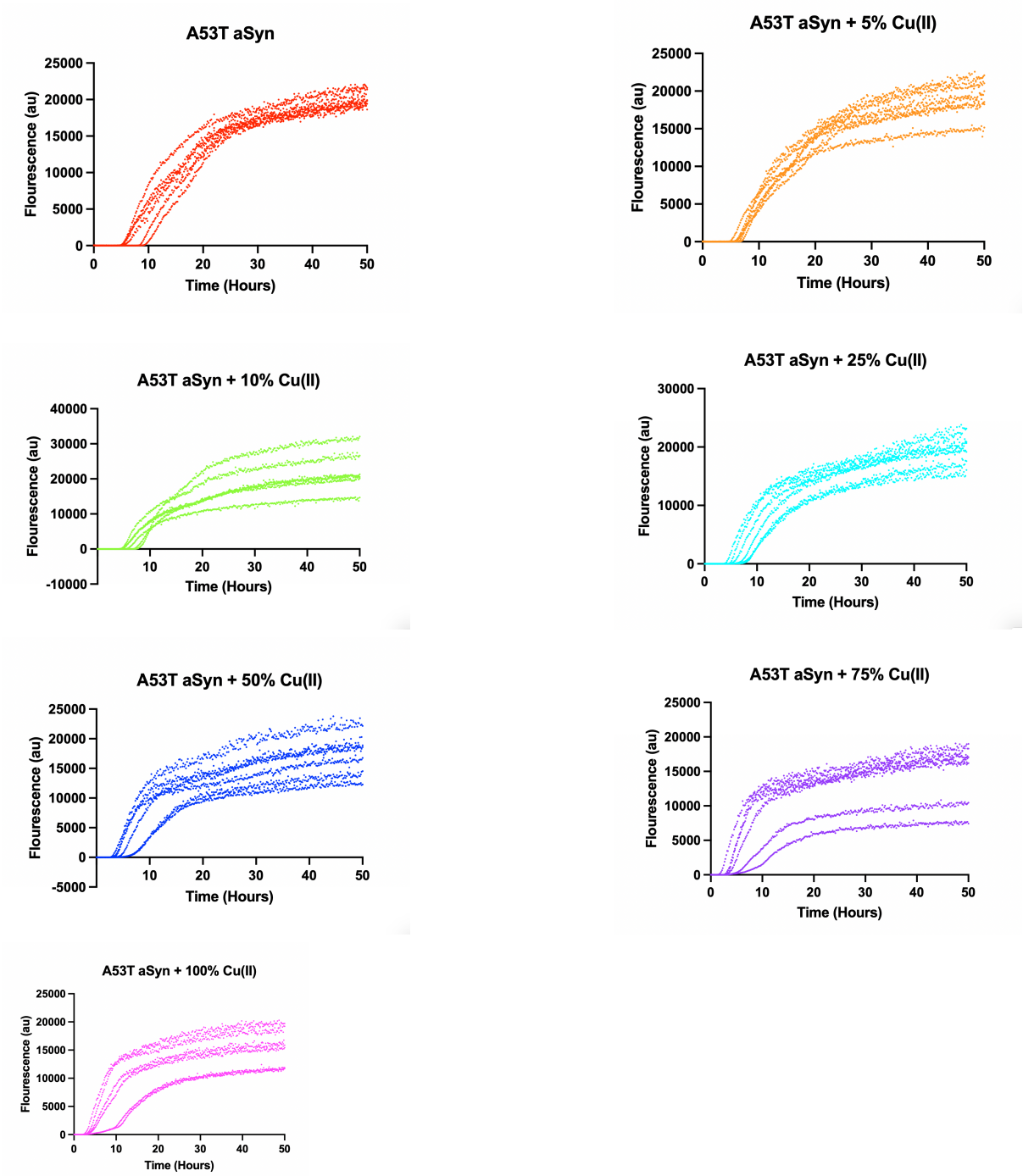

Figure 14: ThT aggregation kinetics with A53T alpha-synuclein and Cu(II). Each dot represents one of the samples fluorescence measurement at a specific time based on the y and x axis.